EFFECT OF FUEL FILM DEPOSITION ON COMBUSTION PROCESS IN PFI SI ENGINE

S. S. Merola, P. Sementa, C. Tornatore, B. M. Vaglieco

Istituto Motori – CNR, Via G. Marconi
8 – 80125 Napoli (Italy)

Abstract

The present paper discusses the experimental investigations on the flame induced by fuel film deposition ignition in a single cylinder, ported fuel injection, four-stroke, over-boosted spark-ignition engine with a four-valve production head. The engine was optically accessible and equipped with a transparent quartz window in the bottom of the combustion chamber. 2D-digital imaging and UV-visible natural emission spectroscopy were used to follow the flame propagation in the combustion chamber. Two colour pyrometers were applied to evaluate flame temperature and soot concentration. Particulate matter and soot primary particles diameters were measured and correlated with the soot amount produced in the combustion chamber. The effect of the intake air pressure and injection phasing was investigated.

Optical setup for spectroscopic measurements and visible digital imaging, visible flame emission detected in the chamber for the selected operating conditions, visible emission spectra measured at 60 CAD ASOS in the chamber, soot concentration measured at the selected operating conditions, integral soot concentration measured at the selected operating conditions, particulate mass concentration measured by the Opacimeter and particles number concentration measured by LII at the engine exhaust are presented in the paper.

Keywords: *Overboosting, Spark Ignition Engine, Optical Diagnostics, Fuel Film Deposition*

1. Introduction

In port fuel injection spark-ignited engines (PFI SI), thin films of liquid fuel can form on the valves surface and on the cylinder walls [1, 6, 14, 17, 20]. Once formed, the fuel films develop dynamically under the influence of gas flow and valve movement and they affect the complexity of the combustion process. In particular, film vaporization and fire near the valves can reduce the flame speed and the complete flame propagation creating locally rich-zones. During the fuel film-evolution process, it is possible to achieve gas temperature and mixture strength conditions that lead to fuel film ignition, creating a diffusion-controlled flame that can persist well after the normal combustion event. Just before the opening of the exhaust valves, this flame produces soot which cannot be completely oxidized due to the too low temperatures in the cylinder. Chamber locations where the fuel-air mixture is too lean to burn are a particular concern for unburned hydrocarbon emissions. Thus, the fuel film burning leads to increased smoke and hydrocarbons emissions [4].

The aim of this paper was to study the overboosting and injection phasing influence on the fuel film formation and burning. Moreover, the effect of the diffusion-controlled flame near the valves and the cylinder walls on nanoparticles emission at the exhaust was evaluated.

The measurements were performed in a single cylinder, port fuel injection, four-stroke spark-ignition engine with a four-valve production head. Optical techniques based on 2D-digital imaging were used to follow the flame propagation in the combustion chamber. Natural emission spectroscopy was applied to detect the radical species that are markers of combustion and soot precursors. Two-colour pyrometry was employed to measure the soot temperature and concentration. Laser Induced Incandescence technique applied at the undiluted exhaust allowed the measurement of primary particles size and number concentration.

2. Experimental apparatus

The engine used is an optically accessible single cylinder port fuel injection spark ignition engine with a displacement of 399 cm^3 and a compression ratio of 10:1. More details on the engine are reported in [12]. A specially machined cylinder head of a four valve commercial automotive engine was used. The engine was equipped with an external overboosting system that allowed the choice of the flow mass, the temperature and the pressure of the intake air. The in-cylinder pressure was measured for every engine cycle by a piezo-electric pressure transducer.

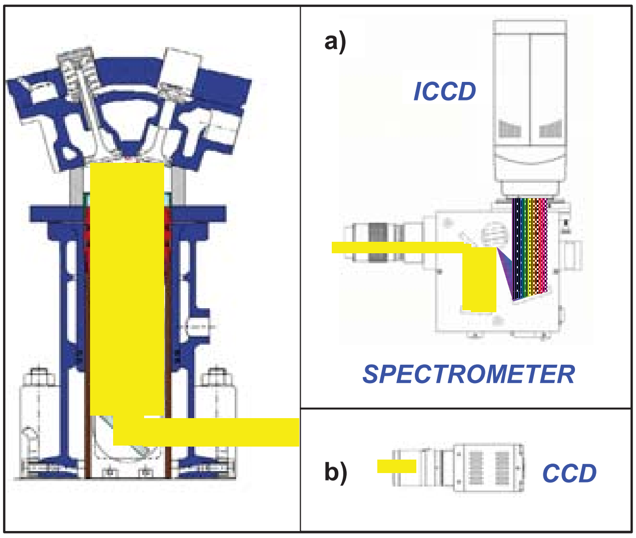

Fig. 1. Optical setup for (a) spectroscopic measurements and (b) visible digital imaging

Figure 1 shows the experimental setup for spectroscopic measurements and digital imaging. During the combustion process, the emitted light passed through the quartz window located in the piston and it was reflected toward the optical detection assembly by a 45° inclined quartz mirror. The mirror had an elliptical shape (47 x 66 mm). More details on the engine are reported in [12].

For the spectroscopic investigations the combustion light emission was focused by a 78 mm focal length, f/3.8 UV Nikon objective onto the micrometer controlled entrance slit of a spectrometer with 150 mm focal length, f/3.8 aperture, 300 groove/mm grating (Fig. 1a).

2D soot flame visualization was obtained by digital CCD colour camera system and a 50 mm focal length, f/3.8 Nikon lens (Fig. 1b). The optical assessment allowed a spatial resolution around 0.1 mm/pixel. Spatial distribution of soot temperature and concentration was obtained by the two colour method. The soot-emission wavelengths were selected by edge filters. More details about this methodology are reported in [18, 19].

For all optical measurements, the synchronization between the CCD and ICCD cameras and the engine was made by the Crank Angle Encoder signal through a Delay Unit. The CCD and ICCD cameras exposure time was fixed at 41.6 μs. The cameras were not cycle resolved detectors. In this work, each image was detected at a fixed crank angle of different engine cycles. The dwell time between two consecutive images was set at 41.6 μs.

2.3. Exhaust measurements

2.3.1. Laser Induced Incandescence

The basic principle of Laser Induced Incandescence (LII) measurements is to heat up the carbonaceous particles by a highly energetic laser pulse from ambient temperature and to analyse the enhanced thermal radiation [16]. The primary particles size has a strong effect on the cooling rate of the soot particles to the local gas temperature. The difference between the particle surface temperature and the ambient gas decays steadily in an exponential manner. With the determination of the characteristic decay time, primary particles diameter may be calculated [10].

The measurements were carried out on the undiluted exhaust exciting by the first harmonic (1064 nm) of Q-switched Nd:YAG laser. More details about the LII optical setup are reported in [2]. The LII signal was focused by a 15 cm focal length lens on the input window of a gated intensified camera (ICCD). It was placed at 90° angle to the direction of the incident beam. The detection wavelength was 430 nm with a bandwidth of 10 nm FWHM.

The ICCD received an external timing signal from the Nd:YAG pump laser and it detected the LII signal just 10 ns after the laser pulse. The ensemble decay curve was obtained by moving the gate via software. From the LII signal curve, the temperature decay and the characteristic decay time were determined, thus the primary particle diameter was obtained. In order to reduce the statistical uncertain, every spectrum was obtained as accumulation of 50 consecutive spectra.

2.3.2. Exhaust gas and particulate measurement system

Steady-state measurements of CO, CO_2, O_2, HC and NOx were made in the raw exhaust by AVL analyzers. CO, CO_2 and HC were measured by Non-Dispersive Infrared Detectors (NDIR); NOx and O_2 were detected by means of electrochemical sensor. An Opacimeter was used to measure particulate mass concentration. Opacimeter is a partial-flow system that measures the visible light attenuation (550 nm) from the exhaust gases. From empirical relations it is possible to convert the opacity percentage in particulate mass concentration [15].

3. Engine operating conditions

All the tests presented in this paper were carried out at engine speed of 2000 rpm and full load. The equivalence ratio was fixed at λ=1 and measured by a lambda sensor installed at the engine exhaust. The fuel injection pressure was 3.5 bar more than the boost pressure. Intake air pressure values of 1000 and 1400 mbar were considered. Closed and open valve injection conditions were investigated at fixed intake air pressure. More details about the engine operating conditions and exhaust emissions are reported in Table 1.

Tab. 1.Engine operating conditions and exhaust emissions

Phasing Condition	Absolute Intake Air Pressure [mbar]	Spark Timing vs. TDC [CAD]	Duration of Injection [CAD]	Start of Injection vs. TDC [CAD]	Fuel [kg/h]	CO [%]	CO_2 [%]	HC [ppm]
Closed valves	1000	-24	90	130	1.7	0.4	13.4	485
Open valves	1000	-24	90	-300	1.7	0.6	14.0	537
Closed valves	1400	-14	130	130	2.7	0.3	13.7	515
Open valves	1400	-14	130	-300	2.7	0.3	14.6	376

Pressure measurements were performed for all the selected operating conditions. The rate of chemical energy release and related parameters such as IMEP were evaluated on an individual cycle basis and/or averaged on 400 cycles from the cylinder pressure data using conventional interpretation models for heat release analysis [7].

It is known that in-cylinder pressure signal is influenced by cycle-to-cycle variation and by heat transfer due to the quartz window [19]. The heat exchange of different components of the optical engine induced a thermal evolution and cycle-to-cycle variation of maximum pressure signal. Table 2 reports the IMEP and related Coefficient of Variation (COV) evaluated on 400 cycles from the cylinder pressure data.

Tab. 2. Indicated Mean Effective Pressure and Coefficient of Variation

Absolute Intake Air Pressure [mbar] – injection phasing	IMEP [bar]	COV [%]
1000 - closed valves	8.3	1.6
1000 - open valves	8.3	1.8
1400 - closed valves	13.0	2.7
1400 - open valves	13.0	3.6

4. Results and discussions

Figure 2 reports the flame visible emission revealed in the engine cylinder for the selected operating conditions reported in Tab.1. The images are representative of combustion late phases. For both intake air pressure values in the closed-valve injection condition a diffusion-controlled flame, named pool fire, was observed especially near the intake valves. On the other hand, in the open-valve injection conditions the intake valve firing phenomenon was not evident. A flame emission weaker than the closed-valve case was detected near the cylinder walls and the exhaust valve region.

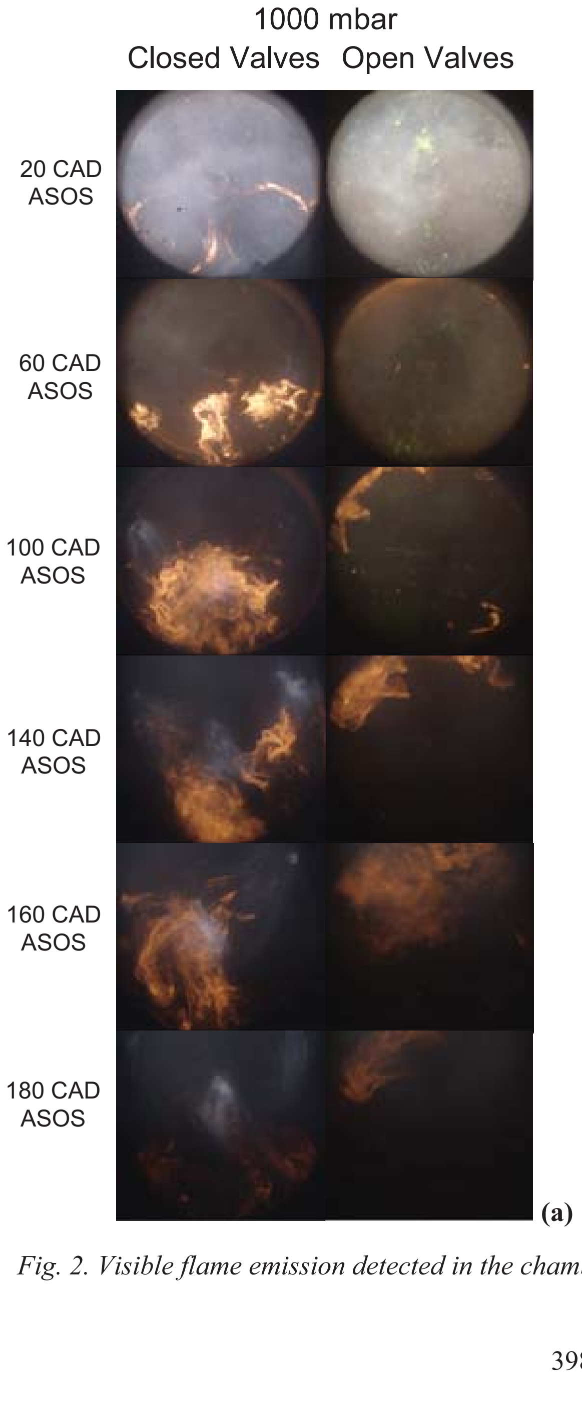

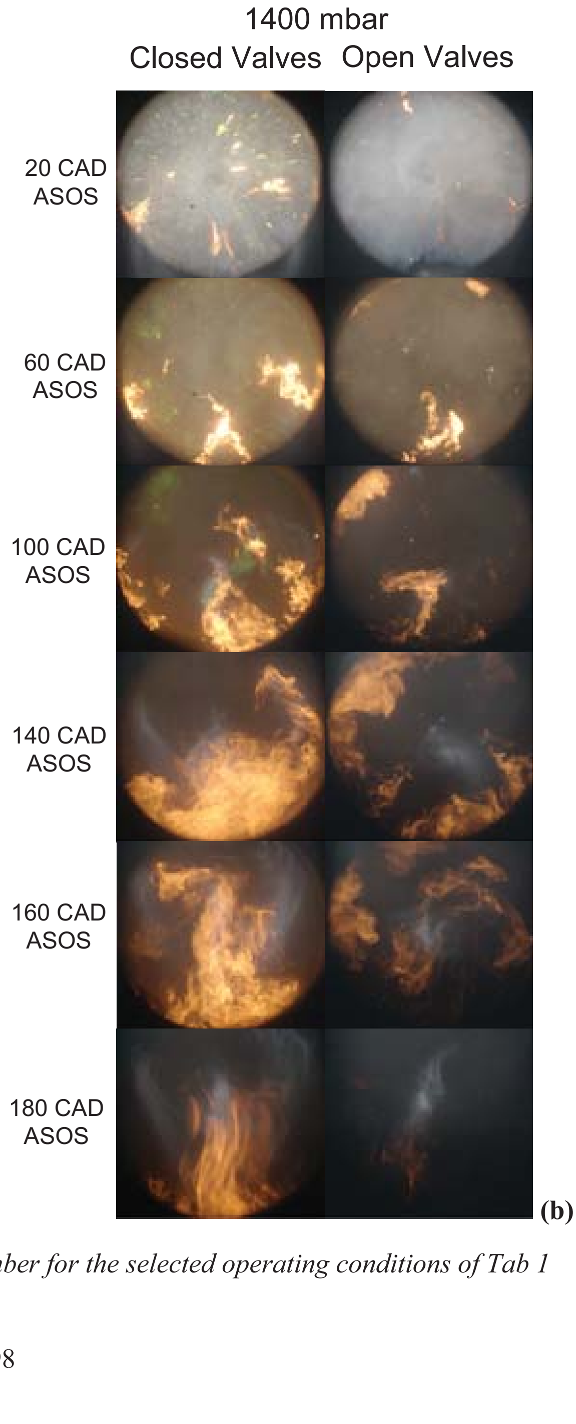

Fig. 2. Visible flame emission detected in the chamber for the selected operating conditions of Tab 1

In order to identify the chemical species occurring during the valve and walls firing, spectroscopic investigations of natural emissions were performed in different locations of the chamber. Figure 3 reports the spectra detected in two typical locations of the combustion chamber at 60 CAD ASOS for the overboosted-closed valve injection condition. Location A was closed to the centre and B was between the intake valves.

The reported spectra show a band centred at 309 nm due to OH radical [5]. OH is widely present in the chamber during all the combustion process; it is marker of high temperature combustion and chemical reactions. Moreover, in location A, CO-O and soot precursors-spectral features were detected [8]. Spectra measured in the location B were characterized by a strong continuous contribution that increased with the wavelength in the visible range. This was typical of blackbody emission due to the soot particles.

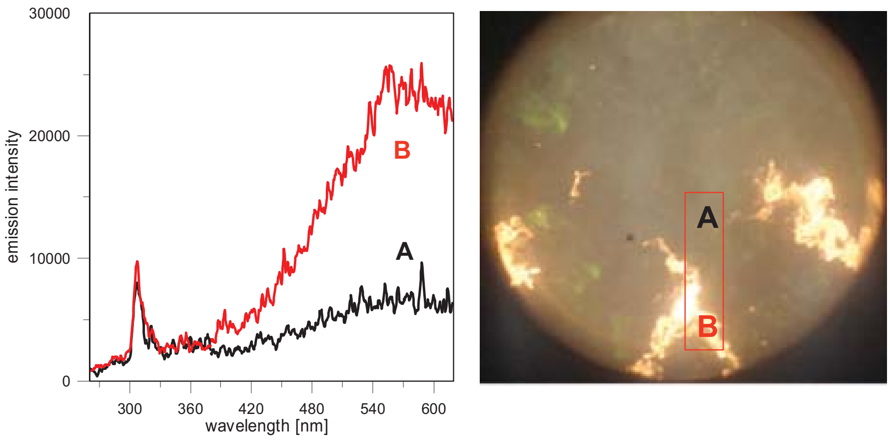

Fig. 3.UV- Visible emission spectra measured at 60 CAD ASOS in the chamber locations A and B

In order to study the effect of valve firing on soot time and spatial evolution, two-colour pyrometry was applied. Figure 4 reports soot concentration measured at the selected operating conditions (Tab. 1) and Figure 5 shows the evolution of the integral soot concentration.

At each intake air pressure, the soot evolution was dependent on the injection phasing even if the same fuel amount was injected. In good agreement with the previous flame emission results (Figure. 2), in closed valves conditions the soot was formed in the intake valves region. On the other hand, in open valves conditions the major source of soot was the diffusion flame generated by the fuel deposition on the cylinder walls.

For 1000 mbar-intake air pressure, in the closed-valve injection condition soot concentration was higher than the open-valve injection condition until few CAD before the exhaust valves opening that occurred at 153 CAD ATDC (Figure 5a). Then, an inversion of tendency was observed. At the exhaust valves opening, higher particulate mass concentration was emitted in the open valve injection condition; this was due to a low soot reduction rate observed in this configuration. In the overboosted case, the closed-valve injection condition always presented higher soot levels than the open valve injection condition until the opening of exhaust valves.

In conclusion, for the open valve conditions, the higher air injection pressure and turbulence level had a positive effect on the particulate emission. In overboosted condition, in fact, the soot oxidation rate was higher than 1000 mbar-intake air pressure condition due to higher pressure and temperature in the cylinder during the late phase of combustion. The achieved pressure and temperature values promoted a better vaporization of fuel film near the chamber walls and improved the soot burning. For the closed valve injection conditions the overboosting played a negative role on the particulate emission. This was caused by the simultaneous injection of higher amount of fuel (overboosted condition) and the pool fire formation (closed valve condition). The soot reduction rate when the exhaust valves started opening was not sufficient to oxidise the particulate.

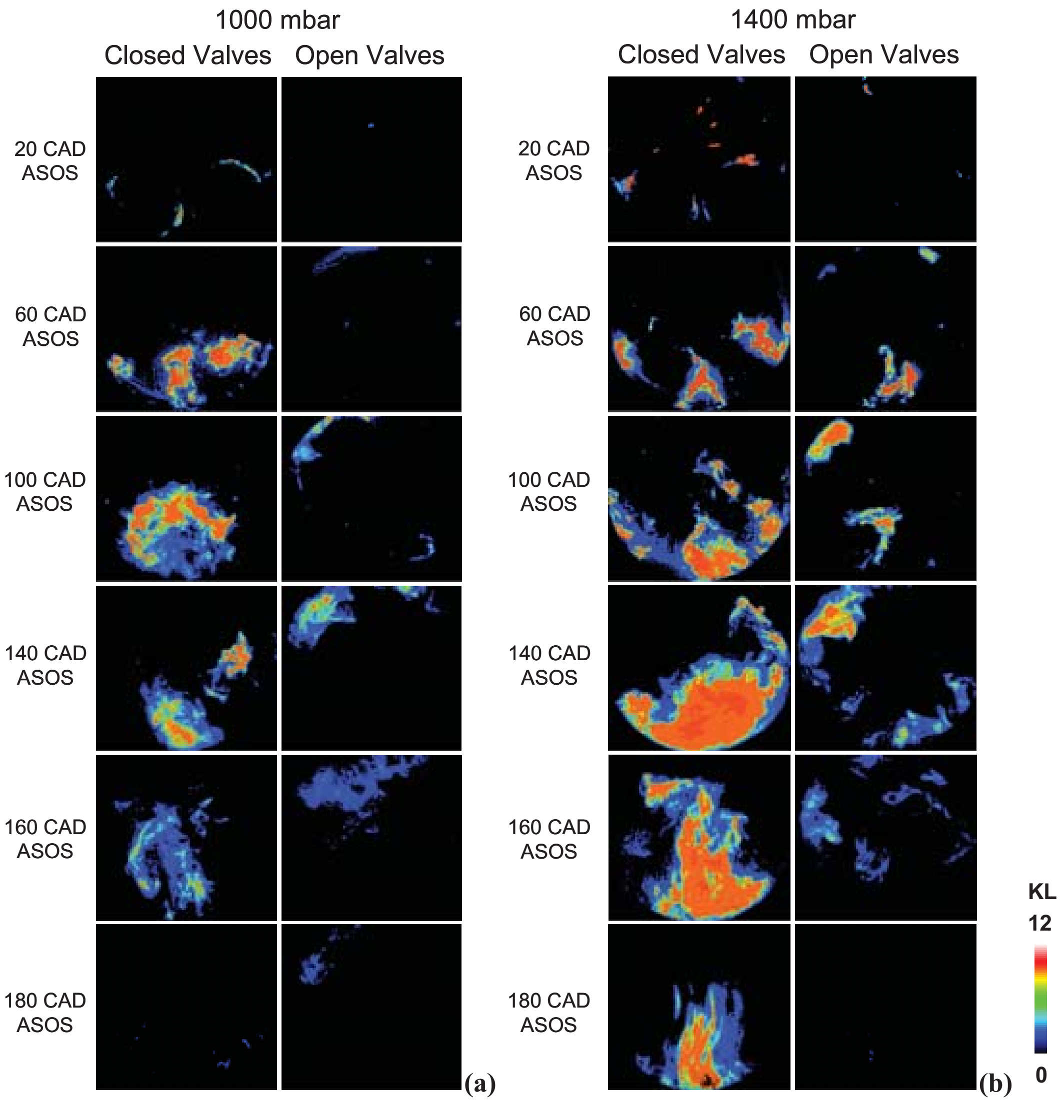

Fig. 4. Soot concentration measured at the selected operating conditions of Tab 1

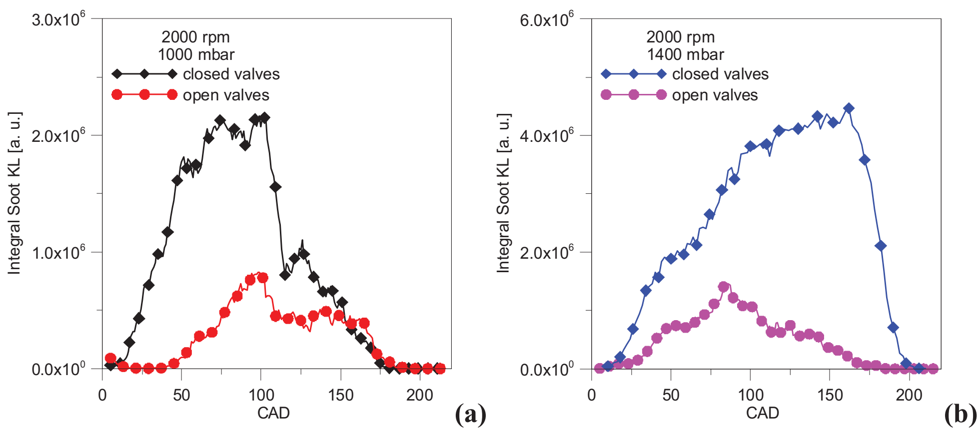

Fig. 5. Integral soot concentration measured at the selected operating conditions of Tab 1

In Figure 6a the particulate mass concentration measured at the engine exhaust is reported. The results were in good agreement with those obtained by in-cylinder measurements.

In order to obtain information about soot particles size and concentration Laser Induced Incandescence technique was applied at the engine exhaust. LII measured high number concentration of primary particles smaller than 30 nm (nanoparticles) was detected; the particles mean diameter was not strongly influenced by the engine operating condition.

As reported in Figure 6b, the number of nanoparticles in 1000 mbar-intake air pressure condition was lower for closed valves injection. In the overboosted case, the injection with open valves induced the formation of a lower amount of nanoparticles. It should be noted that the proposed optical engine lacks of aftertreatment device. On the other hand, as reported in a previous investigation [13], the nanoparticles cannot be removed by three way catalysts. Thus it seems to be necessary to optimise the engine operating conditions taking into account the lowest emissions of nanoparticles. The results reported in this paper are in good agreement with recent experimental studies that demonstrated the presence of high number of nanometric carbonaceous particles at the exhaust of PFI SI engines not only during the cold start-up but also at low speed [3, 9, 11].

a) b)

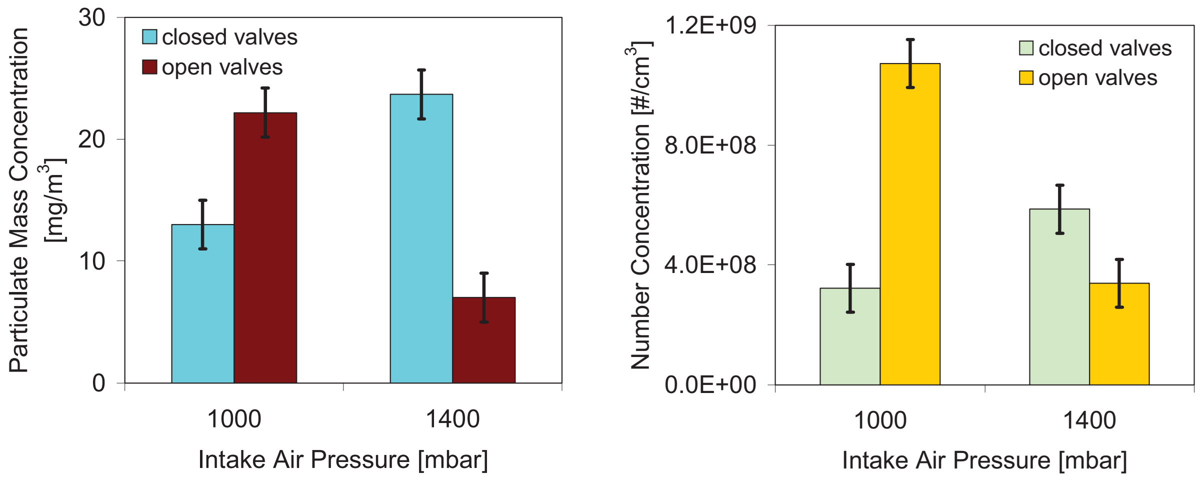

Fig. 6. (a) Particulate mass concentration measured by the Opacimeter and (b) Particles number concentration measured by LII at the engine exhaust

5. Conclusions

The overboosting and injection phasing influences on the fuel film formation/burning and on nanoparticles emission were investigated in a Port Fuel Injection Spark Ignition (PFI SI) engine. The experiments were carried out in a single cylinder, four-stroke optical engine equipped with a four-valve production head.

Optical techniques based on 2D-digital imaging were used to follow the flame propagation in the combustion chamber. Moreover spatial and temporal soot evolution was evaluated by two-colour pyrometry. In the closed-valve injection condition a diffusion-controlled flame was observed near the intake valves. The overboosting played a negative role on the particulate formation and oxidation due to the simultaneous injection of higher amount of fuel (overboosted condition) and the pool fire formation (closed valve condition).In the open-valve injection conditions, a weaker flame emission was detected near the cylinder walls and the exhaust valve region. The overboosting had a positive effect on the particulate amount detected in the combustion chamber. The higher air injection pressure and turbulence level in the intake manifold and the pressure and temperature values achieved in the combustion chamber promoted a better vaporization of fuel film near the chamber walls and improved the soot burning.

Laser Induced Incandescence technique was applied at the engine undiluted exhaust to obtain information about soot particles size and concentration. High number concentration of nanoparticles was detected. The particles mean diameter was not strongly influenced by the operating condition unlike the number concentration. The number of nanoparticles in 1000 mbar-intake air pressure condition was lower for closed valves injection, on the contrary, in the overboosted case, the injection with open valves induced the formation of a lower amount of nanoparticles.

Acknowledgments

The authors thank Mr. Carlo Rossi and Mr. Bruno Sgammato for their precious help and technical support.

References

[1] Costanzo, V. S., Heywood, J. B., *Mixture Preparation Mechanisms in a Port Fuel Injected Engine*, SAE paper n. 2005-01-2080, 2005.

[2] Di Iorio, S., Merola, S. S., Vaglieco, B. M., Tornatore, C., *Diesel Exhaust Nanoparticles Characterization by Multiwavelength Techniques, Laser Induced Incandescence and ELPI*, SAE Paper n. 2005-24-021, 2005.

[3] Di Iorio, S., Merola, S. S., Vaglieco, B. M., Tornatore, C., *Nanoparticles Characterization at Spark Ignition Engine Exhaust*, SAE Paper n. 2005-24-010, 2005.

[4] Drake, M. C., Fansler, T. D., Solomon, A. S., Szekely, G. A. Jr., *Piston fuel films as a source of smoke and hydrocarbon emissions from a wall-controlled spark-ignited direct- injection engine*, SAE Paper n. 2003-01-0547, 2003.

[5] Gaydon, A. G., *The Spectroscopy of Flames*, Chapman and Hall ltd., 1957.

[6] Gold, M. R., Arcoumanis, C., Whitelaw, J. H., Gaade, J.; Wallace, S., *Mixture Preparation Strategies in an Optical Four-Valve Port-Injected Gasoline Engine*, Int. J. of Engine Research, Vol. 1, N. 1, 41-56, 2000.

[7] Heywood, J. B., *Internal Combustion Engine Fundamentals*., New York: McGraw-Hill, 1988.

[8] Lipatnikov, A. N., Chomiak J., *Turbulent flame speed and thickness: phenomenology, evaluation and application in multi-dimensional simulations*, Prog.En.Comb. Sci.; 28:1–73, 2002.

[9] Maricq, M., Xu, N., Chase, E., *Measuring particulate mass Emissions with the Electrical Low Pressure Impactor*, J. Aerosol Science and Technology, 40: 68 – 79, 2006.

[10] McCoy, B. J., Cha, C. Y., *Transport Phenomena in the Rarefied Gas Transition Regime*, Chemical Engineering Science, v. 29, pp.381-388, 1974.

[11] Merola, S. S., Vaglieco, B. M., Di Iorio, S., *Nanoparticles at Internal Combustion Engines Exhaust: Effect on Urban Area*, SAE Paper n. 2006-01-3006, 2006.

[12] Merola, S. S., Vaglieco, B. M., *Knock investigation by flame and radical species detection in spark ignition engine for different fuels*, Proc. ECOS2006 Conference, paper n. 230, 2006.

[13] Merola, S. S., Vaglieco, B. M., *Optical Investigations of Valve Firing in PFI Spark-Ignition Engine*, Proc. ECOS 2007 Conference, Paper n° ECOS07-M01 – Volume I, page 105, 2007.

[14] Meyer, R., Heywood, J. B., *Liquid Fuel Transport Mechanisms into the Cylinder of a Firing Port-Injected SI Engine During Start Up*, SAE Paper n. 970865, 1997.

[15] Mörsch, O., Sorsche, P., (DaimlerChrysler AG*) Investigation of Alternative Methods to Determine Particulate Mass Emissions,* http://www.oica.net/htdocs/Main.htm

[16] Schraml, S., Will, S., Leipertz, A., *Simultaneous Measurement of Soot Mass Concentration and Primary Particle Size in the Exhaust of a DI Diesel Engine by Time-Resolved Laser-Induced Incandescence (TIRE-LII)*, SAE Paper n. 1999-01-0146, 1999.

[17] Shin, Y., Cheng, W. K., Heywood, J. B., *Liquid Gasoline Behaviour in the Engine Cylinder of a SI Engine*, SAE Paper n. 941872, 1994.

[18] User manual firm of AVL, AVL Graz, Austria 2003.

[19] Zhao, H., Ladommatos, N., *Engine Combustion Instrumentation and Diagnostics*, SAE Int., Inc. 2001.

[20] Zhu, G. S., Reitz, R. D., Xin, J., Takabayashi, T., *Modelling Characteristics of Gasoline Wall Films in the Intake Port of Port Fuel Injection Engines*, Int. J. of Engine Research, Vol. 2, N. 4, 231-248, 2001.